U.S. Department
of Transportation

**Federal Railroad
Administration**

Full-Scale Locomotive Dynamic Collision Testing and Correlations: Offset Collisions between a Locomotive and a Covered Hopper Car (Test 4)

Office of Railroad
Policy and Development
Washington, DC 20590

DOT/FRA/ORD-11/16.II

Final Report
September 2011

NOTICE

This document is disseminated under the sponsorship of the Department of Transportation in the interest of information exchange. The United States Government assumes no liability for its contents or use thereof. Any opinions, findings and conclusions, or recommendations expressed in this material do not necessarily reflect the views or policies of the United States Government, nor does mention of trade names, commercial products, or organizations imply endorsement by the United States Government. The United States Government assumes no liability for the content or use of the material contained in this document.

NOTICE

The United States Government does not endorse products or manufacturers. Trade or manufacturers' names appear herein solely because they are considered essential to the objective of this report.

REPORT DOCUMENTATION PAGE

Form Approved
OMB No. 0704-0188

1. AGENCY USE ONLY (Leave blank)	2. REPORT DATE	3. REPORT TYPE AND DATES COVERED
	September 2011	Technical Report

4. TITLE AND SUBTITLE

Full-Scale Locomotive Dynamic Collision Testing and Correlations: Offset Collisions between a Locomotive and a Covered Hopper Car (Test 4)

5. FUNDING NUMBERS

6. AUTHOR(S)

Gopal Samavedam and Kash Kasturi

7. PERFORMING ORGANIZATION NAME(S) AND ADDRESS(ES)

Foster-Miller, Inc.
350 Second Avenue
Waltham, MA 02451-1196

8. PERFORMING ORGANIZATION REPORT NUMBER

DFRA.040048

9. SPONSORING/MONITORING AGENCY NAME(S) AND ADDRESS(ES)

U.S. Department of Transportation
Federal Railroad Administration
Office of Railroad Policy and Development
1200 New Jersey Avenue, SE
Washington, DC 20590

10. SPONSORING/MONITORING AGENCY REPORT NUMBER

DOT/FRA/ORD-11/16.II

11. SUPPLEMENTARY NOTES

Program Manager: John Punwani

12a. DISTRIBUTION/AVAILABILITY STATEMENT

This document is available to the public through the FRA Web site at http://www.fra.dot.gov.

12b. DISTRIBUTION CODE

13. ABSTRACT (Maximum 200 words)

This report presents the test results and finite element correlations of a full-scale dynamic collision test with rail vehicles as part of the Federal Railroad Administration's research program on improved crashworthiness of locomotive structures. This test involved the 30-mile per hour oblique collision of a locomotive with a stationary covered hopper car fouling the locomotive's right-of-way. The test used an SD70-MAC locomotive.

The locomotive and the cars in its consist were fully instrumented with accelerometers, strain gauges, and anthropomorphic test dummies. High-speed photography was used to record the events.

This report presents the test data and the dynamic finite element modeling results. Reasonable agreement has been found in the dynamic event sequence correlations and the structural damage to the front end of the locomotive.

14. SUBJECT TERMS	15. NUMBER OF PAGES
Full-scale tests, locomotive collision post, dynamic finite element analysis, locomotive crashworthiness, anthropomorphic test dummy	44
	16. PRICE CODE

17. SECURITY CLASSIFICATION OF REPORT	18. SECURITY CLASSIFICATION OF THIS PAGE	19. SECURITY CLASSIFICATION OF ABSTRACT	20. LIMITATION OF ABSTRACT
Unclassified	Unclassified	Unclassified	

NSN 7540-01-280-5500

Standard Form 298 (Rev. 2-89)
Prescribed by ANSI Std. 239-18
298-102

METRIC/ENGLISH CONVERSION FACTORS

ENGLISH TO METRIC	METRIC TO ENGLISH
LENGTH (APPROXIMATE)	**LENGTH (APPROXIMATE)**
1 inch (in) = 2.5 centimeters (cm)	1 millimeter (mm) = 0.04 inch (in)
1 foot (ft) = 30 centimeters (cm)	1 centimeter (cm) = 0.4 inch (in)
1 yard (yd) = 0.9 meter (m)	1 meter (m) = 3.3 feet (ft)
1 mile (mi) = 1.6 kilometers (km)	1 meter (m) = 1.1 yards (yd)
	1 kilometer (km) = 0.6 mile (mi)
AREA (APPROXIMATE)	**AREA (APPROXIMATE)**
1 square inch (sq in, in^2) = 6.5 square centimeters (cm^2)	1 square centimeter (cm^2) = 0.16 square inch (sq in, in^2)
1 square foot (sq ft, ft^2) = 0.09 square meter (m^2)	1 square meter (m^2) = 1.2 square yards (sq yd, yd^2)
1 square yard (sq yd, yd^2) = 0.8 square meter (m^2)	1 square kilometer (km^2) = 0.4 square mile (sq mi, mi^2)
1 square mile (sq mi, mi^2) = 2.6 square kilometers (km^2)	10,000 square meters (m^2) = 1 hectare (ha) = 2.5 acres
1 acre = 0.4 hectare (he) = 4,000 square meters (m^2)	
MASS - WEIGHT (APPROXIMATE)	**MASS - WEIGHT (APPROXIMATE)**
1 ounce (oz) = 28 grams (gm)	1 gram (gm) = 0.036 ounce (oz)
1 pound (lb) = 0.45 kilogram (kg)	1 kilogram (kg) = 2.2 pounds (lb)
1 short ton = 2,000 pounds (lb) = 0.9 tonne (t)	1 tonne (t) = 1,000 kilograms (kg)
	= 1.1 short tons
VOLUME (APPROXIMATE)	**VOLUME (APPROXIMATE)**
1 teaspoon (tsp) = 5 milliliters (ml)	1 milliliter (ml) = 0.03 fluid ounce (fl oz)
1 tablespoon (tbsp) = 15 milliliters (ml)	1 liter (l) = 2.1 pints (pt)
1 fluid ounce (fl oz) = 30 milliliters (ml)	1 liter (l) = 1.06 quarts (qt)
1 cup (c) = 0.24 liter (l)	1 liter (l) = 0.26 gallon (gal)
1 pint (pt) = 0.47 liter (l)	
1 quart (qt) = 0.96 liter (l)	
1 gallon (gal) = 3.8 liters (l)	
1 cubic foot (cu ft, ft^3) = 0.03 cubic meter (m^3)	1 cubic meter (m^3) = 36 cubic feet (cu ft, ft^3)
1 cubic yard (cu yd, yd^3) = 0.76 cubic meter (m^3)	1 cubic meter (m^3) = 1.3 cubic yards (cu yd, yd^3)
TEMPERATURE (EXACT)	**TEMPERATURE (EXACT)**
[(x-32)(5/9)] °F = y °C	[(9/5) y + 32] °C = x °F

QUICK INCH - CENTIMETER LENGTH CONVERSION

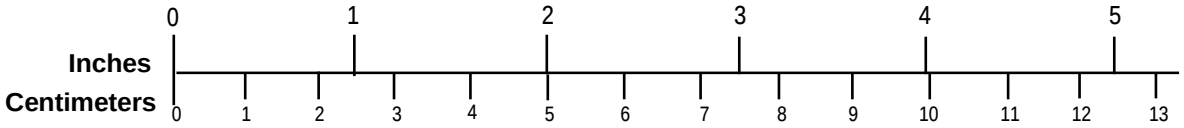

QUICK FAHRENHEIT - CELSIUS TEMPERATURE CONVERSIO

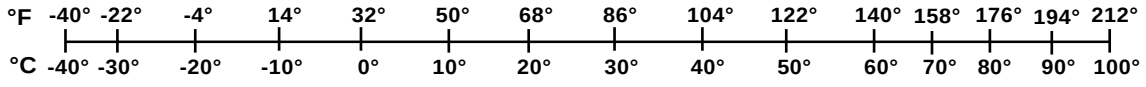

For more exact and or other conversion factors, see NIST Miscellaneous Publication 286, Units of Weights and Measures. Price $2.50 SD Catalog No. C13 10286

Updated 6/17/98

Acknowledgments

This report discusses full-scale rail vehicle collision test and test data correlations with dynamic finite element analysis. Foster-Miller, Inc., performed this work under contract DTFR53-01-D-0029 Task Order 0001 from the Federal Railroad Administration (FRA) for the Locomotive Crashworthiness Research Program.

Mr. John Punwani, FRA Office of Research and Development, is the Contract Officer's Technical Representative. The author thanks Mr. Punwani for his technical direction and involvement in the project.

The support of Ms. Claire Orth, Chief of Equipment and Operating Practices, FRA Office of Research and Development, and that of Dr. Magdy El-Sibaie, Director, FRA Office of Research and Development, is gratefully acknowledged.

The authors would like to express their gratitude to Mr. Gunars Spons for his coordination of the test activities at the Transportation Technology Center. Thanks are also due to Transportation Technology Center, Inc., test personnel, particularly Mr. Russ Walker, Mr. Mark White, and Dr. Barrie Brickle.

The authors want to thank Dr. Bud Zaouk for his help in the final revision of this report.

Contents

Illustrations

Tables

Executive Summary

The Federal Railroad Administration (FRA) initiated the Locomotive Crashworthiness Research Program with the objective of improving crew safety in the event of collisions involving railroad vehicles. This report presents a full-scale dynamic collision test between a moving locomotive consist and a loaded stationary covered hopper car consist fouling the locomotive's right-of-way at a switch. The project team performed full-scale dynamic tests representing common accidents at the Transportation Technology Center (TTC) during this study. This test scenario was selected because it was identified as one of the critical scenarios in the FRA document [1] from which the Transportation Technology Center Institute (TTCI) wrote a test plan and Foster-Miller, Inc., wrote the test requirements definition, conducted the test, and measured structural damage, decelerations, and strains at critical locations. TTCI also captured the response of an instrumented anthropomorphic test dummy (ATD). Foster-Miller correlated results with finite element model (FEM) predictions. The test locomotive was supplied by Sharma and Associates.

This report presents test results including structural damage, decelerations, and strains at critical locations, and the response of an instrumented ATD. This report correlates the FEM predictions with the test data.

In the test, a locomotive (SD70-MAC) with three trailing cars moving at 29.8 miles per hour (mph) sideswiped a stationary covered hopper car consist that contained 30 loaded hopper cars. The impact derailed the front truck of the locomotive and caused substantial damage to the locomotive's right windshield corner post and hood. The stationary covered hopper car also derailed.

Foster-Miller correlated the finite element analysis generated for the side swiping scenario. The simulations reasonably predicted the overall collision dynamic sequences and damages to the locomotive.

The following lessons were learned from this test:

- Locomotive sideswiping generates significant damage to the windshield corner post area of the locomotive.
- This damage would be greater with a larger hopper to locomotive overlap or impact speed.
- Some hood and end-plate damage also occurred.
- The locomotive's front truck derailed, whereas the rear truck remained on the track.

1. Introduction

1.1 Background

FRA initiated a program on improved crashworthiness of locomotives with the objectives of developing S-580 standards [1] based on analysis and testing. The analysis includes dynamic finite element solutions for collisions to be validated by full-scale testing in the field.

This test involved a locomotive that was built to be structurally equivalent to an SD70-MAC. The locomotive consist had three trailing cars moving at 30 mph sideswiping a stationary covered hopper car consist of 30 loaded hopper cars.

1.2 Objectives

The following are the specific objectives of the program:

1. To understand how crew injuries can occur during collisions involving locomotives.
2. To validate LS-DYNA finite element simulations of collision events.
3. To explore potential improvements in locomotive structure to mitigate crew injuries.
4. To conduct the collision test in accordance with previously defined test requirements with details of the collision scenarios, test equipment, measurements, and instrumentation. The measurements should include the dynamic strains in the collision posts and the deceleration levels on the cab floor.
5. To deploy an ATD in the cab for evaluating crew injuries as a result of intrusion, high decelerations, and secondary impacts on the crew.
6. To correlate the finite element results with the test data on the locomotive structure and the ATD responses.

2. Overall Approach

The collision test occurred at TTC in Pueblo, CO. Foster-Miller first performed a preliminary simulation of the test to provide inputs to the test definition

The correlation made between the simulation results and test data is based on dynamic sequence, accelerations, strains, damage to the structure, and injuries to the crew as indicated by the ATD. The test had sufficient photographic, video, and sensor data to support the simulations.

For the test, a total of 5 seconds (s) of data was recorded, starting 1 s before the initial impact and continuing for 4 s after the initial impact. The computer simulations of the collision event were carried out for the first 1 s after initial impact, which was found to be sufficient to capture the major damage to the locomotive structure. The total number of nodes is approximately 40,000 with each node having 6 degrees of freedom.

2.1 Test Methodology

2.1.1 Test Consists and Equipment

Sharma and Associates and the project team built the test locomotive from a used SD-45 without the engine. Its structural members were similar to an SD70-MAC locomotive.

The loaded hopper cars that formed the striking locomotive consist came from existing TTC stock. The project team procured the flatbed trailer and steel coils.

2.1.2 Test Procedures and Instrumentation

The dynamic impact test had an active locomotive to push the striking test consist (locomotive and three loaded hopper cars). It was released from the pushing locomotive at a predetermined speed and location and then it ran along the track into the stationary targets. A detailed test report can be found in *Locomotive Crashworthiness Impact, Test No. 4: Test Procedures, Instrumentation and Data, FRA Draft Report, September 2004*. The report presents results of the test in the form of acceleration, strains, speed, displacements, accelerations, and forces on the ATD, including photographs before and after the test.

TTCI determined the release distance and the speed of the moving consist at release point from a series of speed calibration runs carried out before each test. TTCI measured the speed of the moving consist at impact by using a laser speed trap and a standard radar gun.

The contact of tape switches on the front of the locomotive triggered all of the instrumentation onboard the vehicles. The tape switches were closed by the contact of the locomotive with the anvil vehicle. The data was then saved for 1 s before the trigger and 4 s after the trigger for a total of 5 s worth of data. The test collected data at a rate of 12,800 hertz (Hz) and saved it onto modular data bricks located onboard the vehicles. The data was then downloaded from the data bricks to a computer after the test was complete.

The test instrumentation included strain gauges, accelerometers, and string potentiometers to characterize the behavior of the vehicles during the collisions. TTCI installed the following measurement devices:

- Strain gauges on the collision posts, underframe, and windshield posts to measure the impact loads on these components.
- Three-axis strain gauge rosettes at the base of each collision post to measure the shear at this location.
- Accelerometers at two locations in the locomotive cab and in the hopper car behind the locomotive.
- An instrumented coupler between the locomotive and the first hopper car to measure the force transferred between the two vehicles.
- String potentiometers between the locomotive and first hopper car to measure the relative three-dimensional displacements of the two vehicles during the collision.

This test used five high-speed film cameras and six standard video cameras to record each impact test.

2.1.3 Test Measurements

TTCI measured the vehicle geometries, the weight of all the moving and stationary consists, and the positions of all the transducers before the test. TTCI provided detailed drawings with the geometry dimensions of the flatbed car and the container, and their relative positions and settings. TTCI recorded weather conditions just before each test.

Strain and acceleration were measured during the test using an onboard data acquisition system, with all data synchronized with a time reference corresponding to the moment of impact, as recorded by the tape switches. The system collected a total of 5 s of data, 1 s before impact and 4 s after impact. Test data was recorded at a sample rate of 12,800 Hz. An SAE J211 [4] filter digitally filtered acceleration data after test data collection at frequencies of 1,000, 100, and 25 Hz. Foster-Miller used only 25- and 60-hertz data in the comparisons.

The following describes measured items for each test.

Test Locomotive Speed

A laser speed trap and an off-board handheld Doppler RADAR Speed Gun (± 0.1 mph) measured the speed of the test locomotive just before impact.

Collision Post Strain

Single axis strain gauges on collision posts measured strain in the longitudinal direction. The following convention was used for rosette strain gauges installed on collision posts:

- Right collision post: Direction 1 = Vertical
  Direction 2 = Diagonal
  Direction 3 = Longitudinal
- Left collision post: Direction 1 = Longitudinal
  Direction 2 = Diagonal
  Direction 3 = Vertical

Figure 1 shows the locations of the strain gauges on the left and right collision post. Gauges 1 through 5 are uniaxial in the longitudinal direction; gauges 6 through 10 consist of three-arm

rosette gauges with measurement in the longitudinal, vertical, and a third diagonal arm in the same plane.

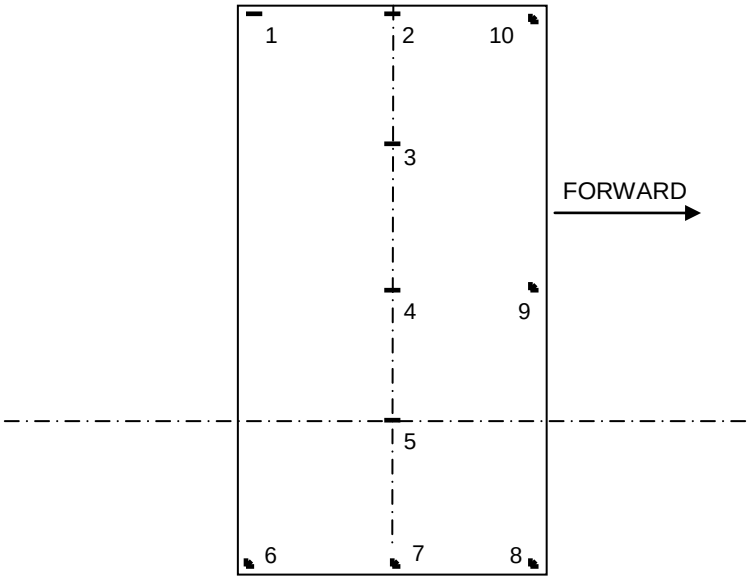

Figure 1. Location of Strain Gauges on the Collision Post

Longitudinal Strain on the Underframe

Figure 2 shows the locations of the strain gauges on the locomotive's underframe. Gauges on the underframe are all uniaxial in the longitudinal direction.

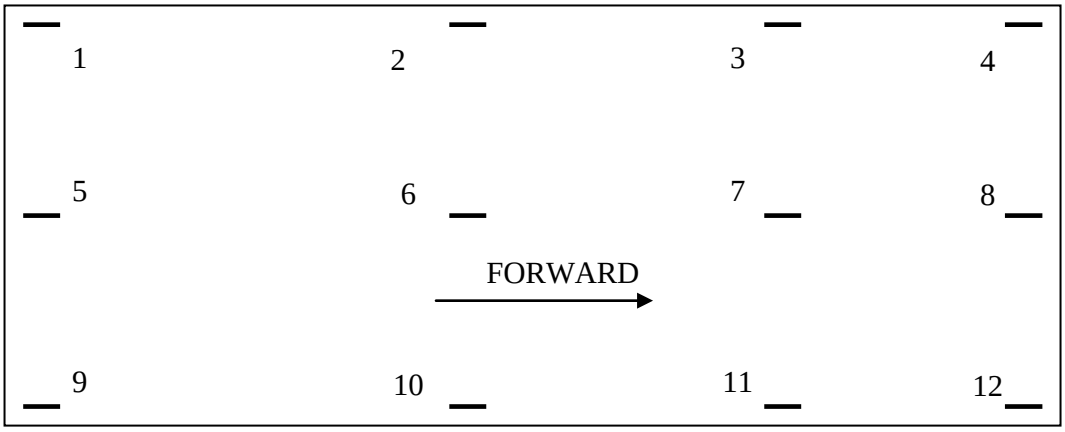

Figure 2. Locations of Strain Gauges on the Underframe

Vertical Strain at the Center Post of the Windshield

Figure 3 shows the location of the strain gauges on the center post of the windshield.

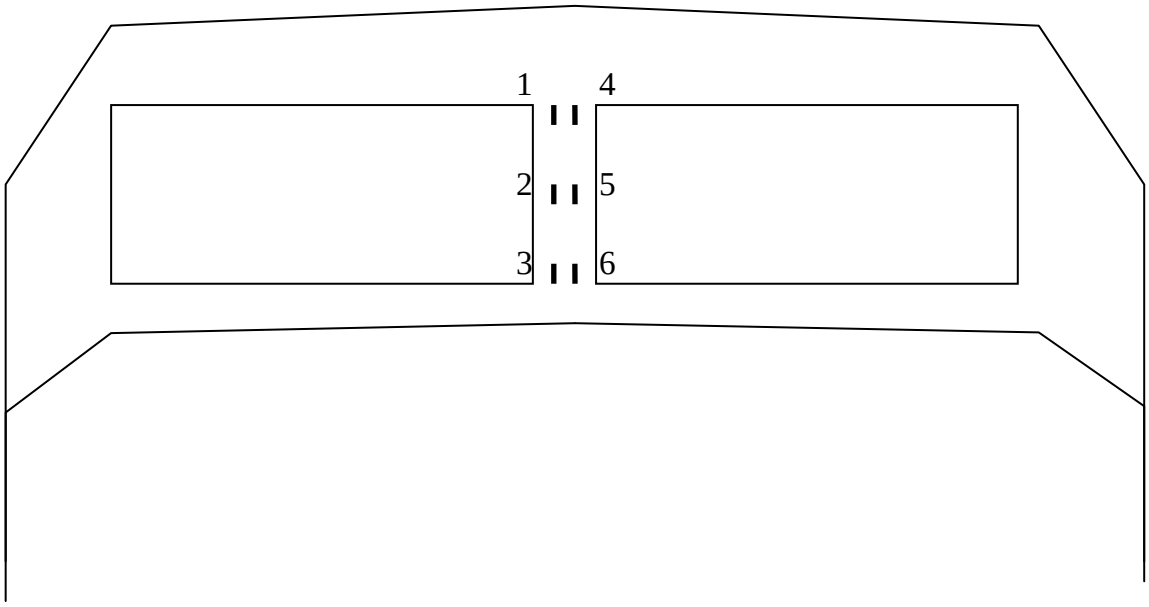

Figure 3. Location of Strain Gauges on Center Post of the Windshield

Additional Strain Measurements

The test recorded measurements for longitudinal strain of the coupler between the moving locomotive and first hopper car.

Acceleration

The test recorded acceleration measurements on the cab floor of the locomotive and on the first two moving hopper cars. TTCI placed a triaxial accelerometer on the floor of the cab, near the driver's seat, to measure the gross and flexible motions of cab floor. Triaxial accelerometers at center sill and at the centerline (axially and laterally) of the first two hopper cars in the moving consist measured the gross and flexible motions of the hopper cars. Additional triaxial accelerometers at various other locations were used to record more data for the three test scenarios.

Table 1 lists the accelerometer locations, accelerometer types, and measured acceleration components for the test scenarios.

Table 1. Typical Locomotive and Hopper Car Accelerometers

Location	Accelerometer	Measurement	
Locomotive floor	Three axis	Longitudinal	X
		Lateral	Y
		Vertical	Z
Locomotive floor (redundant)	Three axis	Longitudinal	X
		Lateral	Y
		Vertical	Z
First moving hopper car	Three axis	Longitudinal	X
		Lateral	Y
		Vertical	Z
Second moving hopper car	Three axis	Longitudinal	X
		Lateral	Y
		Vertical	Z
First stationary hopper car	Three axis	Longitudinal	X
		Lateral	Y
		Vertical	Z
Second stationary hopper car	Three axis	Longitudinal	X
		Lateral	Y
		Vertical	Z
Locomotive, above event recorder	Three axis	Longitudinal	X
		Lateral	Y
		Vertical	Z

The test recorded the acceleration at a sample rate of 12,800 Hz. An SAE J211 filter digitally filtered data at the frequencies of 25 and 60 Hz. The following sign conventions were used for accelerometers:

- X-axis is longitudinal, with positive toward the impact end of the locomotive (forward).
- Y-axis is lateral, with positive toward the right side when facing in the + x-direction (rightward).
- Z-axis is vertical, with positive down toward the ground (downward).

ATD Accelerations and Forces

The test used instrumented ATDs to measure head and chest accelerations and the forces in the neck and femur. Table 2 shows ATD instrumentation locations, type of instrumentation, and measurement orientation. An ATD was seated at the engineer's console in the cab only for this test.

Table 2. ATD Instrumentation

Location	Transducer	Measurement	
Head	Three-axis accelerometer	Longitudinal	X
		Lateral	Y
		Vertical	Z
Chest	Three-axis accelerometer	Longitudinal	X
		Lateral	Y
		Vertical	Z
Upper neck	Six-axis load cell	Longitudinal	X
		Lateral	Y
		Vertical	Z
		Roll	
		Pitch	
		Yaw	
Femur	Two single-axis load cells	Longitudinal (left)	X
		Longitudinal (right)	X

Photography and Video

Five high-speed film cameras and six standard video cameras recorded each collision. Camera coverage was selected to provide views of both the left and right sides of the vehicles, overhead views, and an overall view of the impact. TTCI mounted one of the standard video cameras inside the cab of the locomotive to observe the behavior of the ATD during the collisions.

2.2 Modeling Methodology

To simulate the test scenario and reproduce the behavior of the striking and anvil vehicles throughout the collision process in the test, the following structural models were developed:

- Locomotive
- Loaded hopper cars
- Track system

The models have the following characteristics:

- Appropriate basic structural and mechanical components (including the locomotive, trailing cars, separate bogies and suspension, and draft gear) using shell, plate, beam, and solid finite elements.
- Masses.
- A simplified model simulated the test scenario. The model was defined to represent the entire moving consist and the first three hopper cars of the stationary target consist and a maximum of four vehicles in each consist at the front end of the collision point. Additional masses, suspension, and draft gear stiffness in the remainder of the model represented the full 35 hopper car consist.

- A realistic nonlinear spring rate between the vehicles to represent the effects of draft gear deformations, travel stops, and clearance.
- Nonlinear material property for all deformable structures, with elastic, elasto-plastic, and fully ductile (if applicable) behavior up to fracture (ultimate strength).
- Ground interaction by an orthogonal friction matrix, which considers high friction values transverse to wheel rotation and low values in the line of rolling motion.

The models were developed using HyperMesh™ [2], a multipurpose computerized mesh generator and modeling tool, to generate geometry and mesh models for preprocessing. LS-DYNA [3], a dynamic structural analysis finite element program, was used to perform all simulations. The advantages of using LS-DYNA include the following:

- It is most suitable for analyzing structures in a single process by combining the dynamic modeling of the locomotive consist as a whole with embedded detailed models of the lead locomotive and the objects with which it collides, including standing car consists.
- Simulations permit visualization of the collision process in the early stages where:
  - Most significant locomotive structural deformations, movements, and decelerations occur.
  - Interactions of the locomotive's various components in three dimensions, including the cab and the interior influence crew survivability.
- Models can be developed with detailed representation of the locomotives, rail vehicles, and other potential colliding objects, such as intermodal containers, hopper cars, International Standards Organization containers, and vehicles.

2.2.1 Structures and Dimensions

The locomotives used in the test were an SD-70 MAC type, fabricated by modifying an SD-45 to satisfy the AAR 1990 S-580 crashworthiness standards. Appropriate metal sheet thickness, masses, and inertia in the model represented the actual locomotive used in the real test. The locomotive weighed 380,000 pounds (lb). The model contained either two or three loaded hopper cars (each weighing approximately 260,000 lb) depending on the test to the rear of this locomotive.

Foster-Miller modeled the standing hopper consists (each weighing approximately 270,000 lb) as a four-car consist. Extra weight and a stiff spring were added to the last car to account for the resistance supplied by the remaining 31 cars used in the actual test, thus representing a total of 35 hopper cars.

2.2.2 Boundary Condition and Constraints

Foster-Miller simulated the interaction between the structures (locomotive, hopper cars, trucks, and truck trailers) and ground as friction force. The friction coefficient in the transverse direction of the wheels was assigned to be 0.6, whereas in the rolling direction, it was taken as 0.3.

To improve the simulation of the contact between the locomotive and the stationary hopper car, the model simulated some parts in greater detail (e.g., the front axle of the front locomotive

truck). The model also included the vertical beams on the impact end of the stationary hopper car to improve the contact representation. The spring rate of the couplers was tailored to provide the correct impact momentum to the locomotive. Modeling of these contact interfaces is important for a proper simulation.

2.2.3 Loading Condition

The loads applied in the simulations include the initial moving consist velocities and gravity forces. The velocities of the test locomotive recorded immediately before impact were the initial simulation velocity values.

2.3 Correlation of Simulation and Test Results

This report compares the simulation results with the test data in terms of dynamic event sequences, accelerations, and strain. Simulations predict the first 1 s of the crash event, starting immediately after impact. The accelerations calculated from simulations were filtered by using an SAE J211 filter at 25- and 60-hertz frequencies in a postprocessing program of LS-DYNA. Results after the filtration with the corresponding test data filtered at the same frequencies.

2.3.1 Dynamic Event Sequence

Foster-Miller compared the dynamic event sequence obtained from the collision simulation with photographic and video information from the test. The following dynamic events were used for the test and simulation correlations.

- Deformation to major structural components
- Relative positions of the locomotive and impacted target vehicles
- Component failure

2.3.2 Acceleration

TTCI collected acceleration data at certain locations for comparison with simulation data. The acceleration of the corresponding nodes on the model created simulated output for comparison with test data. In areas without fine mesh modeling, nodes were identified to closely match the accelerometer location. A selected filter first filtered the simulated accelerations and then converted to the unit of g (acceleration due to gravity). Sign conventions for the accelerations are as follows:

- Longitudinal: positive is forward acceleration.
- Lateral: positive is rightward acceleration.
- Vertical: positive is downward acceleration.

Table 3 describes the nodes identified for simulation accelerations and shows the simulation values for comparison with measured test data accelerations.

Table 3. Node Locations Identified for Acceleration

Location	Node Flagged	Comparison
Locomotive floor	Near driver's seat	Longitudinal X
First moving hopper car	Center of centerline at center sill	Longitudinal X
Second moving hopper car	Center of centerline at center sill	Longitudinal X

2.3.3 Strain

Table 4 lists the identified locations for strain correlation. Foster-Miller identified elements on the model at the strain gauge locations in the test. Positive values show tension, and negative values show compression.

Table 4. Strains Identified for Correlation

	Identified Location	Vectors	Strain Gauges in Test
Collision post (left and right)	3	Longitudinal	Standard
	5	Longitudinal	Standard
	8	Vertical	Rosette
	10	Vertical	Rosette
Underframe	6	Longitudinal	Standard
	8	Longitudinal	Standard
Center post of windshield	1	Vertical	Standard
	6	Vertical	Standard

2.3.4 Video

The impact test was visually recorded with five high-speed film cameras and six video cameras. Camera coverage was selected to provide views of both the left and right sides of the vehicles, an overall view of the impact, and included a video camera in the cab of the locomotive. Figure 4 shows the film and video camera locations for the test.

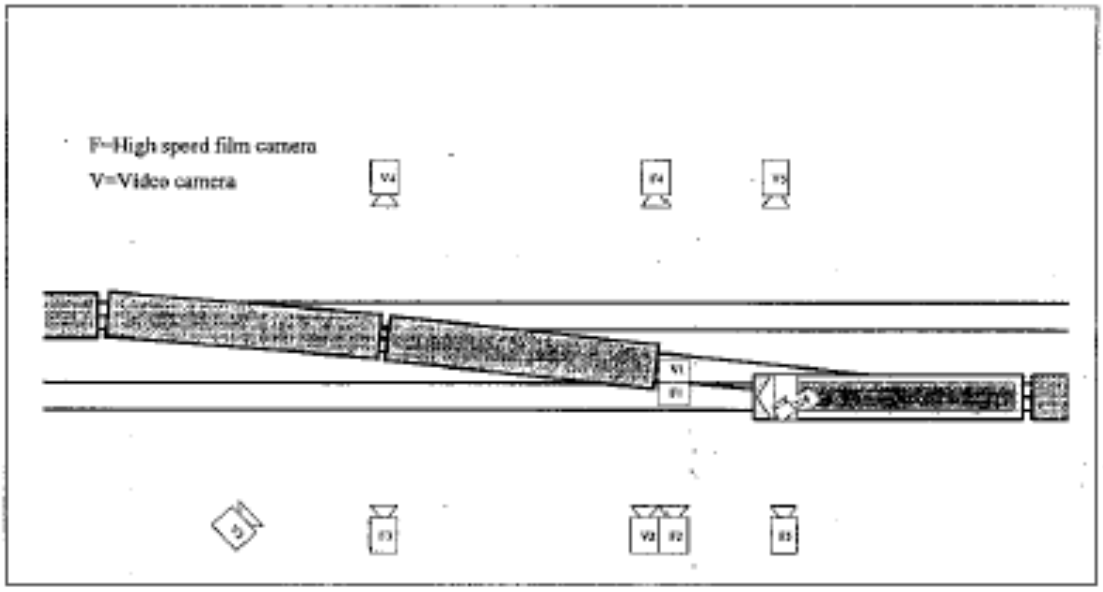

Figure 4. Video Camera Positions

3. Test 4: Locomotive Offset Collision with a Covered Hopper Car

3.1 Test Setup and Collision Damage

The test used a moving consist with a speed of 29.8 mph with the leading SD70-MAC locomotive and three loaded hopper cars as the striking vehicle. The stationary consist, beginning with a covered hopper partially fouling the right-of-way of the oncoming locomotive, had a total of 30 loaded mixed-duty cars, most of which were open-top hopper cars. Figure 5 shows the test setup, and Figure 6 shows the bullet consist before impact. Figure 7 shows the covered hopper car and the target consist.

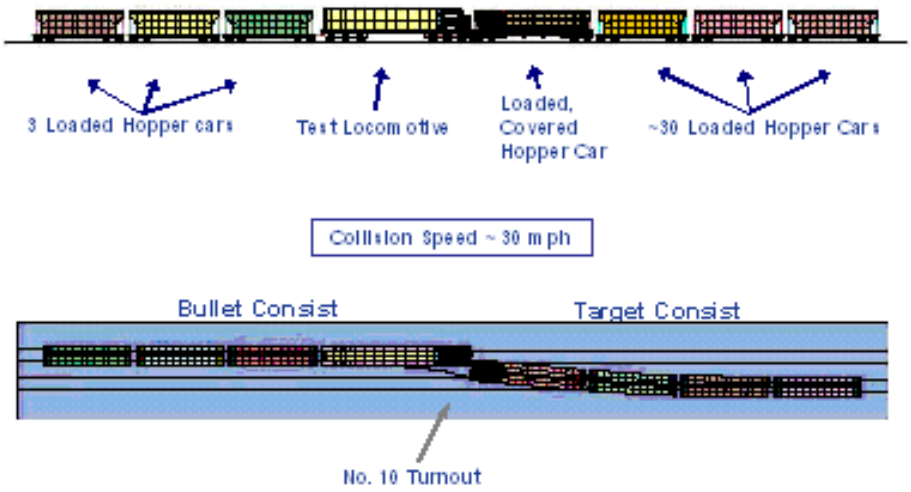

Figure 5. Test Setup

Figure 6. Locomotive and Bullet Consist before Impact Test

Figure 7. Covered Hopper Car and Target Consist before Impact Test

Figure 8 depicts the alignment of the locomotive and covered hopper car at the point of impact. The covered hopper car sits on a turnout connecting the locomotive's rail path to a parallel track, where it fouls the locomotive's right-of-way by approximately 36 inches (in). Figure 9 shows the engineer's view of the covered hopper car while the locomotive was parked during pretest activities.

Figure 8. Alignment of Locomotive and Covered Hopper Car at Point of Impact

Figure 9. View of Covered Hopper Car from Engineer's Seat in Locomotive

Table 5 describes the size and weights of the moving and target consists.

Table 5. Size and Weights of the Test Consists

	Moving Consist		Target Consist	
	Length (ft)	**Weight (lb)**	**Length (ft)**	**Weight (lb)**
Locomotive	70	380,000		
First hopper car	47	263,742		
Second hopper car	49.5	261,876		
Third hopper car	50.8	264,650		
Loaded covered hopper car			54.35	264,581
Total weight		1,170,268		

High-speed video revealed the following dynamic sequences:

- The first contact between the moving locomotive and the stationary covered hopper car occurred when the anticlimber touched and deformed the ladder at the corner of the hopper car (Figure 10). Soon thereafter, the locomotive plow made contact with the hopper side sill and was bent back toward the locomotive end plate. The hopper ladder and locomotive plow, being nonstructural elements, both immediately deformed.

Figure 10. Test at Moment of Impact

- The locomotive vertical end plate made contact with the covered hopper side sill and the horizontal end plate. The side sill was torn away from the horizontal end plate as the left corner of the horizontal end plate was bent downward, making contact with the covered hopper's front truck (Figure 11). The locomotive vertical end-plate sheared off vertically near the draft gear pocket and was bent back underneath the underframe when it came in contact with the front truck. The excessive deformation of the locomotive vertical end-plate caused the plow to completely break free of the end plate.

Figure 11. Locomotive Vertical End Plate Contacts Front Truck

- The deformation and interaction of end-plates and trucks on the two cars was sufficient to form a ramp that lifted and laterally shifted the locomotive's front truck up and to the left. This derailed the truck away from the covered hopper. Simultaneously, the impact compressed the covered hopper's front truck downward and to the right. The lateral forces involved as the locomotive were sufficient to shift the covered hopper rail, causing the covered hopper wheel flanges to slide off the rail. With its front truck derailed, the impact end of the covered hopper shifted approximately 2 feet (ft) from the locomotive and came to rest against the near rail of the parallel track.

- As the end-plate interaction occurred, the locomotive nose made contact with the side and slanting front end of the covered hopper's body (Figure 12). The locomotive nose retained its shape and began to crash into the sloped end of the covered hopper body.

Figure 12. Locomotive Nose Contacts Covered Hopper Body

- The lateral forces at play shifted the locomotive and covered hopper away from one another before the locomotive nose could fully engage the hopper body. This lateral shift, however, caused the upper corner of the hopper body (just above the damaged sloped portion) to align with the locomotive's windshield corner post. The covered hopper corner buckled and tore away the corner post (Figure 13).

Figure 13. Hopper Stiff Corner Contacts Windshield Corner Post

- The wheels of the locomotive's front truck now derailed, landing on the rail ties as the locomotive continued forward at an angle to its direction of travel. The right rear corner of the locomotive contacted the damaged covered hopper, bending the rear vertical end plate (Figure 14).

Figure 14. Locomotive Right Rear Contacts Damaged Covered Hopper Car

- The trailing hopper cars in the bullet consist partially raked the side of the covered hopper car as they passed one another, causing minor damage to the open-top hoppers.
- The bullet consist ultimately came to a stop under the braking action of the three moving hopper cars behind the locomotive.

After the collision, the locomotive came to a stop with its lead truck resting on railroad ties and gravel, having tracked almost one full gauge width to the left after derailing in the collision with the covered hopper. The collision damaged the plow, the right-hand side of the vertical end plate and nose, and the right windshield corner post. Figure 15 shows the derailed, damaged locomotive after impact. Figure 16 provides closeup views of the damage to the windshield corner post, hood, and vertical end plate.

Figure 15. Locomotive after Collision

Figure 16. Damage to Locomotive

Longitudinal translation of the covered hopper car was limited by its being coupled to the remainder of the stationary consist. The collision slightly displaced the second and third stationary cars, which showed damage but did not derail. Figure 17 shows the derailed, damaged covered hopper car after the test. Figure 18 shows the close-up views of the damage of the side sill, horizontal end plate, bolster, and hopper body.

Figure 17. Covered Hopper Car after Collision

Figure 18. Damage to Covered Hopper Car

3.2 Description of the FEM

Figure 19 shows the FEM of the striking locomotive. Figure 20 shows the covered hopper car modeled in detail. Foster-Miller modeled the first three hopper cars in the stationary consist of 30 in detail, as shown in Figure 21. All the remaining cars are combined into a single mass/stiffness system equivalent to the remaining 27 cars. The entire locomotive consist has ~60,000 degrees of freedom.

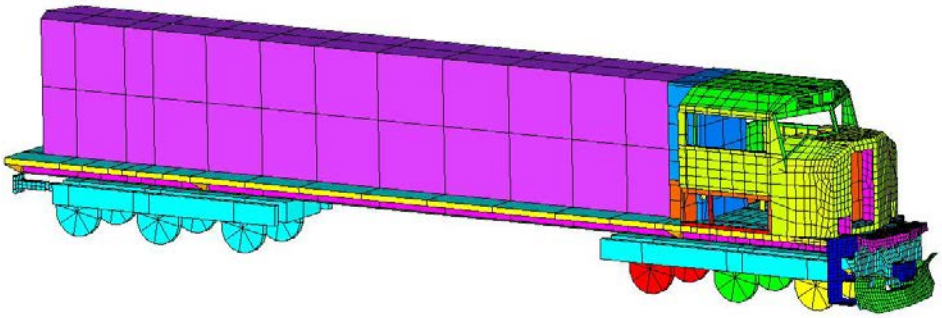

Figure 19. FEM of Bullet Locomotive

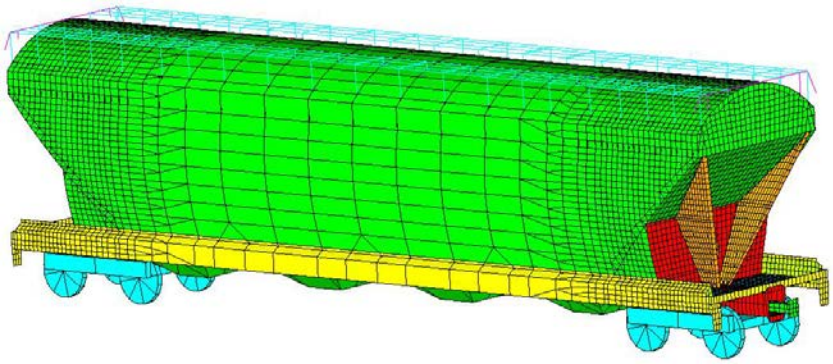

Figure 20. FEM of the Covered Hopper Car

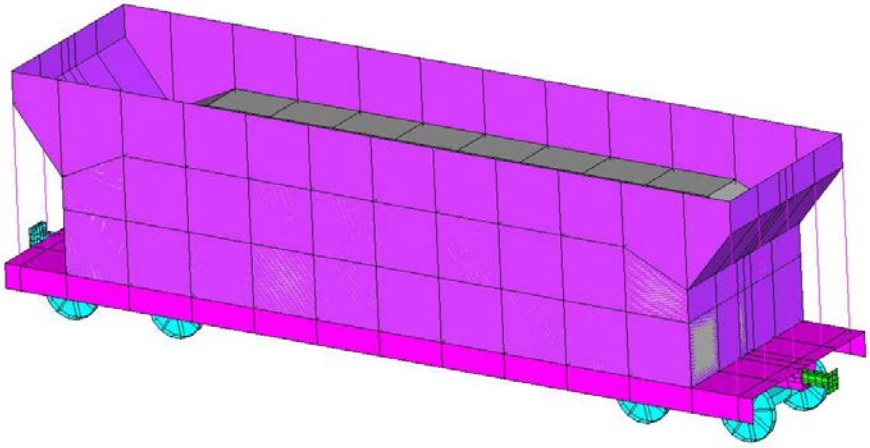

Figure 21. FEM of a General Open-Top Hopper Car

Figure 22 shows the entire model of the Test 4 scenario. Figure 23 depicts the alignment between bullet and stationary consists as the covered hopper car sits on a turnout between parallel sets of tracks.

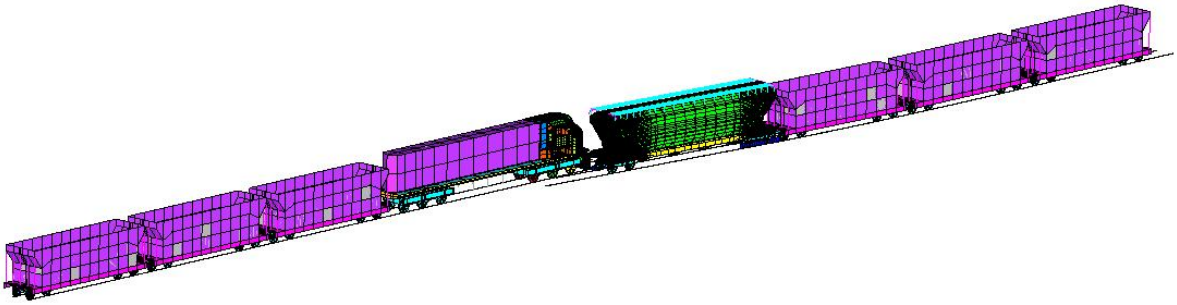

Figure 22. FEM of Test 4

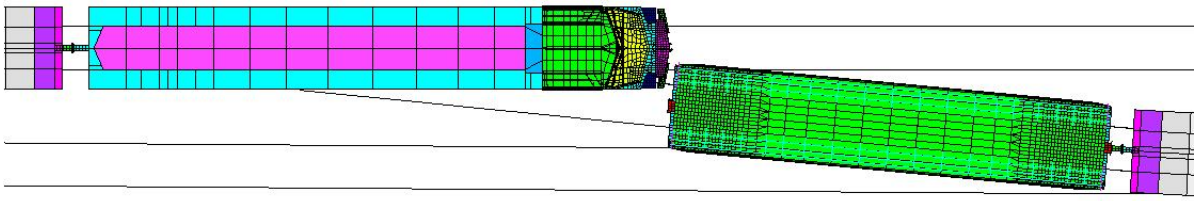

Figure 23. Locomotive and Covered Hopper Alignment in Test 4

3.3 Correlations of the Test Results with the Finite Element Simulation

3.3.1 Dynamic Sequence Correlation

Figure 24 shows the dynamic sequence correlations between the test and the simulation captured at time equals 0.04, 0.225, and 0.64 s. The dynamic sequence as captured from the high-speed video seems to be in reasonable agreement with the simulations from the finite element analysis.

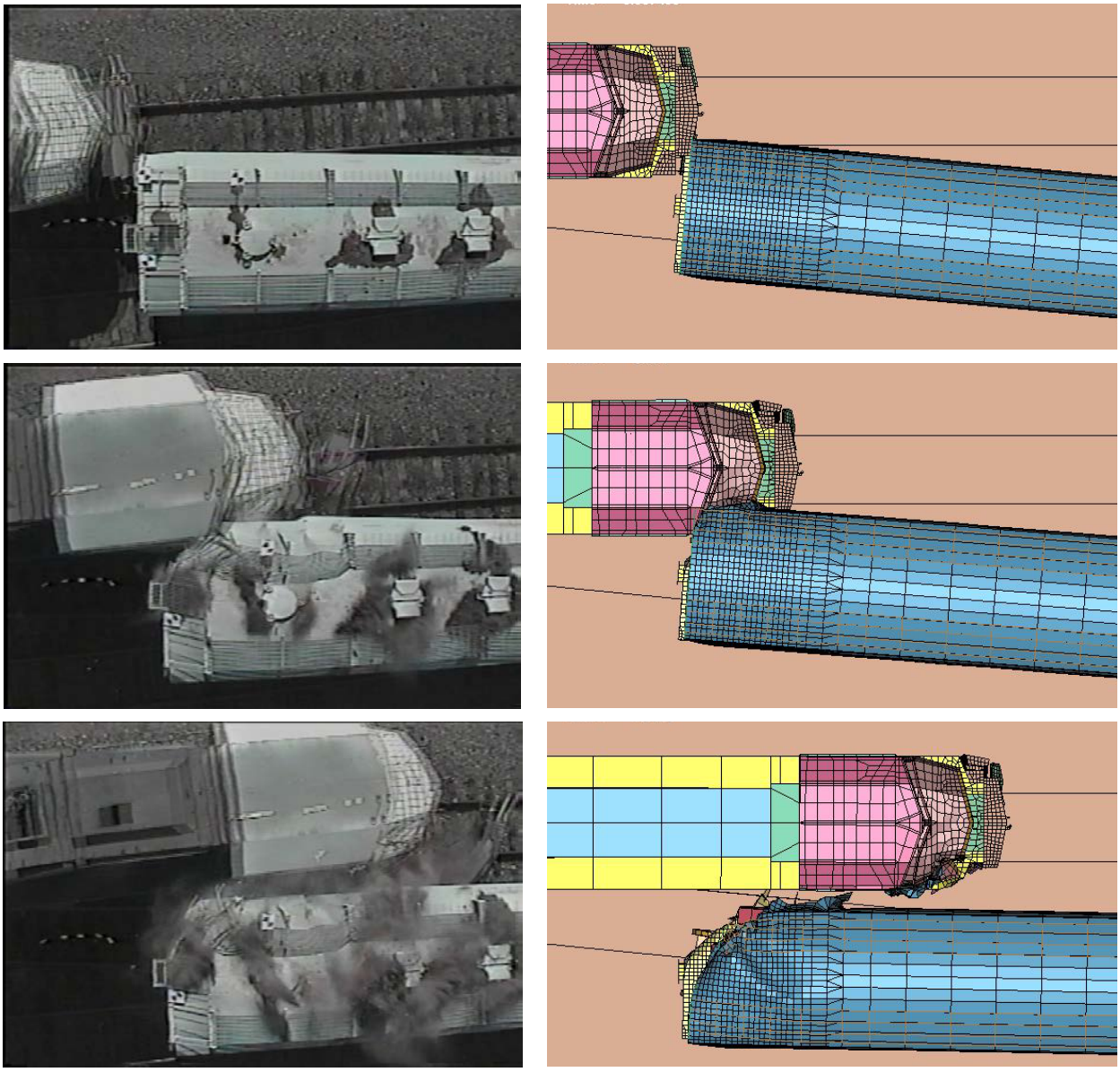

Figure 24. Kinematic Comparison between Test and Simulation

The collision sequence from the simulation was the following:

- The locomotive plow and vertical end plate made contact with the covered hopper's side sill and horizontal end plate. The side sill and horizontal end plate were bent downward,

and the side sill torn open. Figure 25 shows that the left corner of the horizontal end plate was bent downward, making contact with the covered hopper's front truck.

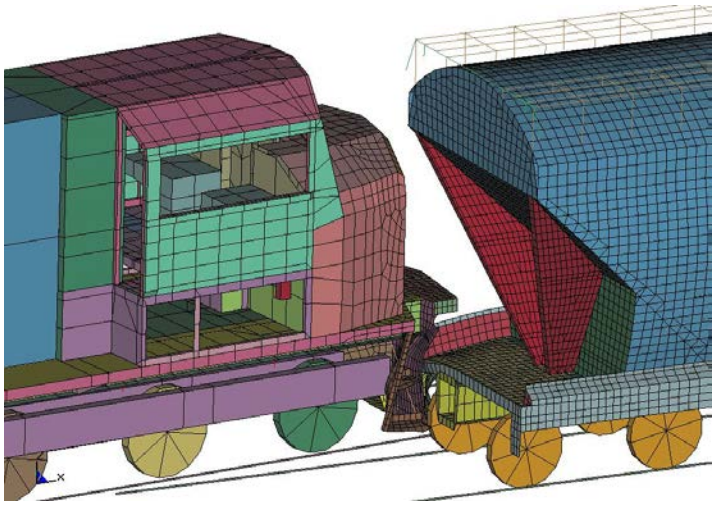

Figure 25. Locomotive and Covered Hopper End Plates in Contact with the Truck

- The locomotive vertical end plate bent back underneath the underframe when it came in contact with the front truck. The locomotive plow was damaged but did not break free from the vertical end plate.
- The deformation and interaction of end plates and trucks on the two cars were sufficient to form a ramp that separated the two cars apart from each other; the locomotive moved to the left, whereas the covered hopper's front truck shifted to the right. Figure 26 shows that the impact end of the covered hopper shifted away from the locomotive as the hood of the locomotive interacted with the body of the covered hopper car.

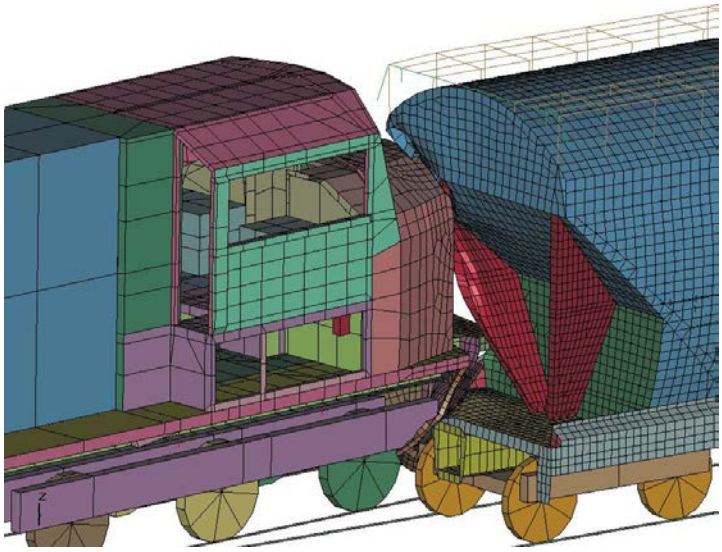

Figure 26. Locomotive Hood in Contact with the Covered Hopper Car

- As the end-plate interaction occurred, the locomotive hood made contact with the sloped end of the covered hopper's body. The locomotive hood was significantly damaged with

plastic deformation at the side of the right collision post. Figure 27 shows that the hopper body side and roof were significantly damaged, exposing the ballast inside the hopper body.

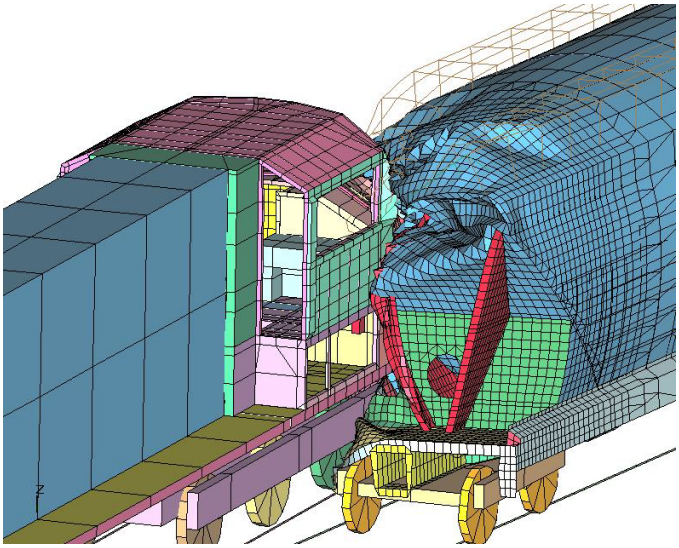

Figure 27. Covered Hopper Car Body Damage

- The lateral forces shifted the locomotive and covered hopper away from one another. This interaction of the locomotive hood and roof with the hopper body moved the covered hopper toward the locomotive. Figure 28 shows that the tangle of hopper body materials tore the locomotive windshield corner post and deformed the side of the locomotive cab.

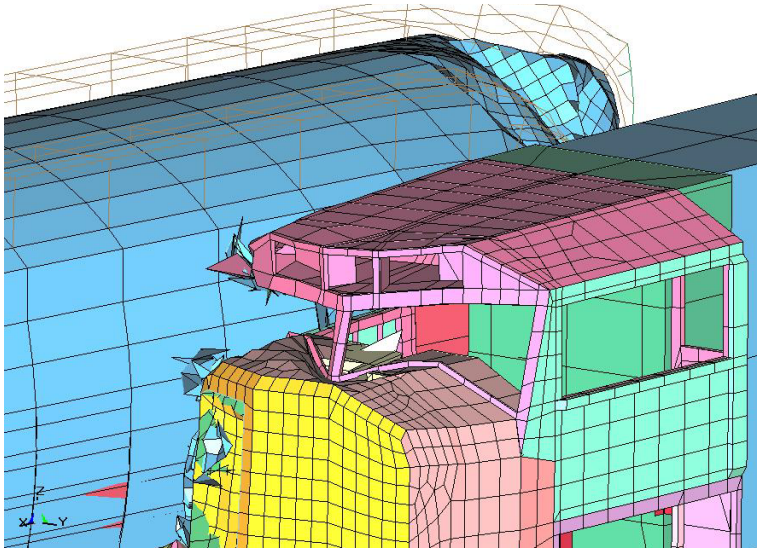

Figure 28. Locomotive Windshield Corner Just after Post Removal

Figure 29 shows the damage to the locomotive and hopper car from the simulated collision.

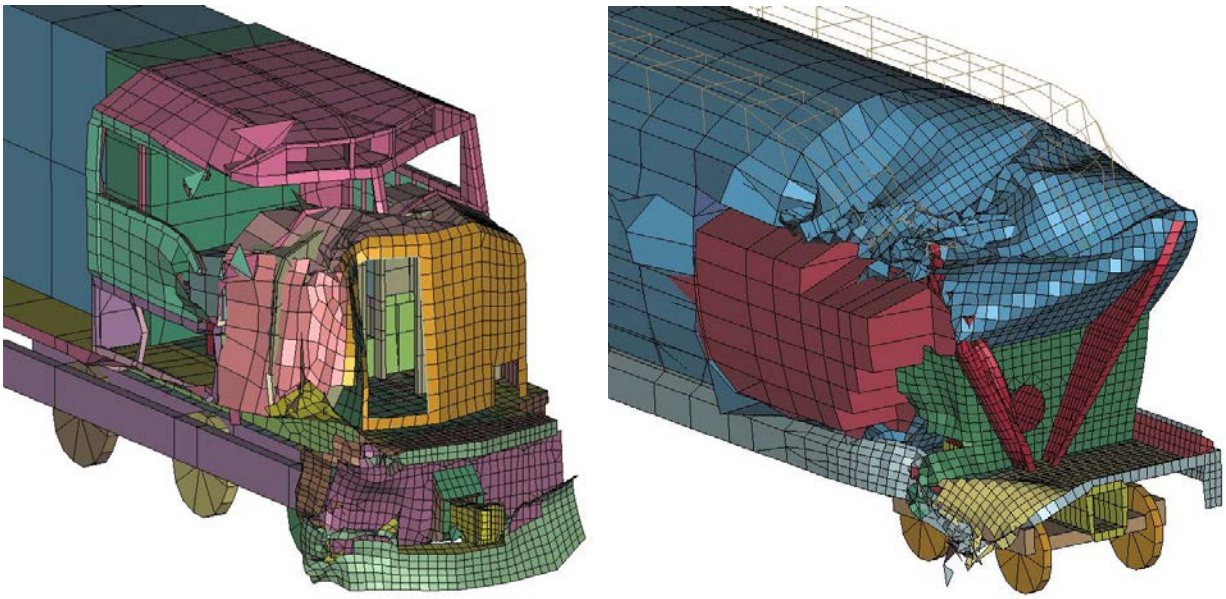

Figure 29. Locomotive and Covered Hopper Car Damage from Simulation

3.3.2 Acceleration Correlation

Acceleration data obtained from the full-scale test were compared with the accelerations obtained from the finite element simulation. Data collected during the test included accelerations of the locomotive floor, the first two moving hopper cars behind the locomotive, and the first two leading stationary hopper cars at the sill level.

Figure 30 shows the acceleration correlations between the test vehicles and the finite element simulation. SAE J211 60-hertz filter was used for structural acceleration data. As shown in the figure, the simulation prediction for longitudinal acceleration of the locomotive cab floor varied from the test accelerations. In addition, the results show that the peak longitudinal accelerations for the cab floor were lower than the predicted values.

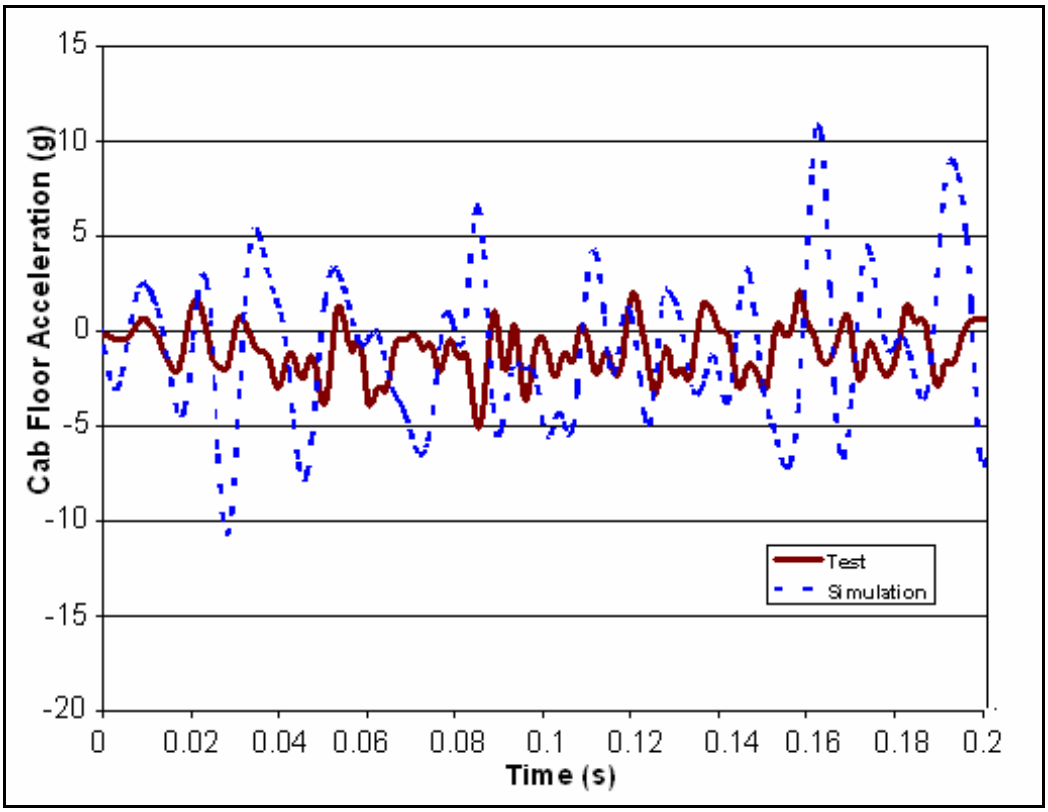

Figure 30. Locomotive Cab Floor Longitudinal Acceleration Filtered at 60 Hz

3.3.3 Strain Correlations

Strain data for collision posts, lead underframe, and the right-hand corner windshield post of the locomotive correlated data between simulation and test. The collision posts and underframe did not suffer any significant damage in the real collision. Simulation results, however, would suggest the occurrence of plastic deformation in the right collision post and surrounding hood structure. The right-hand windshield corner post was torn from the cab in both the test and simulation. Table 4 describes element locations and the identified strains chosen for correlation. Figure 31 through Figure 36 show these strain correlations.

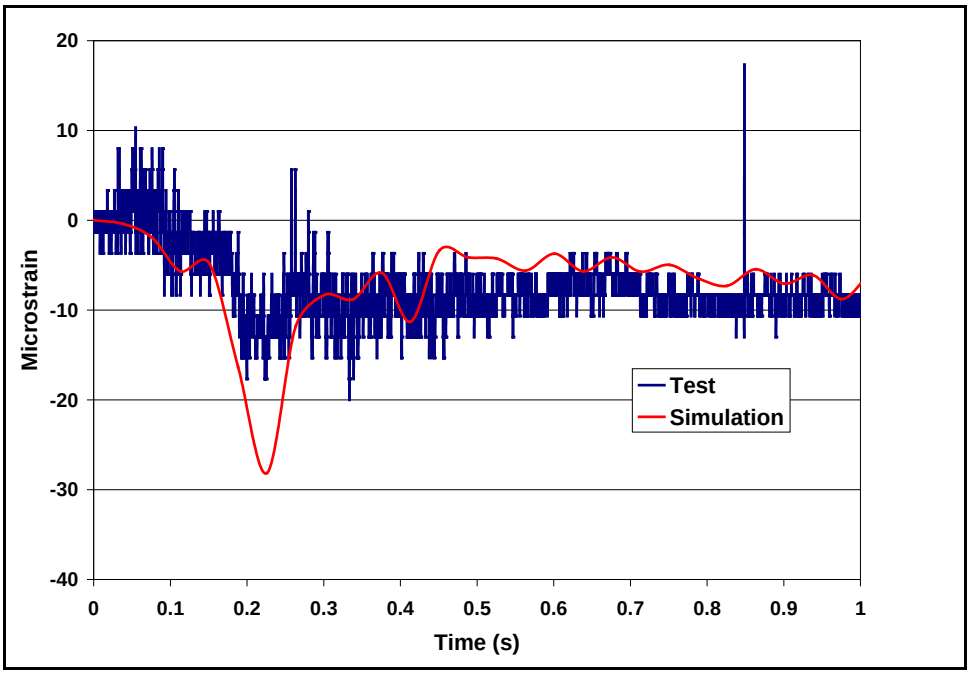

Figure 31. Left Collision Postlongitudinal Strain at Location 1

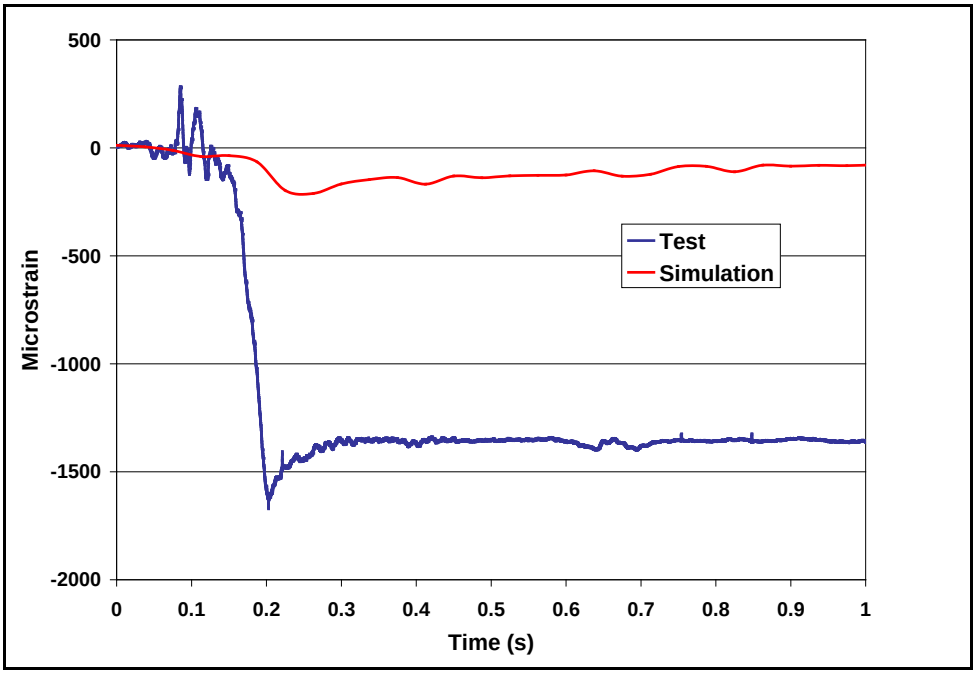

Figure 32. Left Collision Postlongitudinal Strain at Location 10

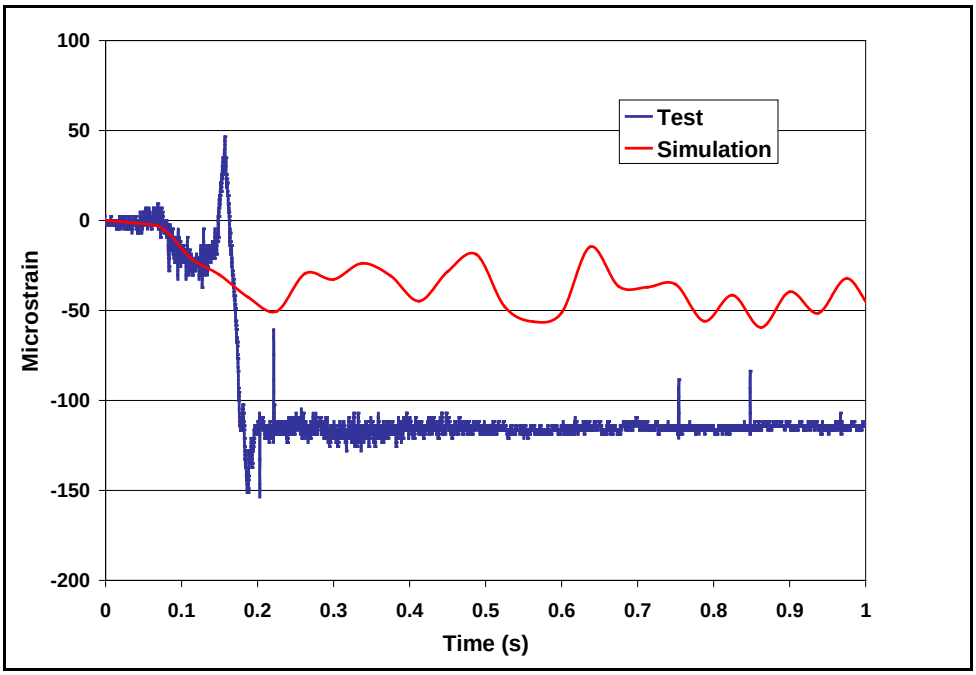

Figure 33. Right Collision Postlongitudinal Strain at Location 1

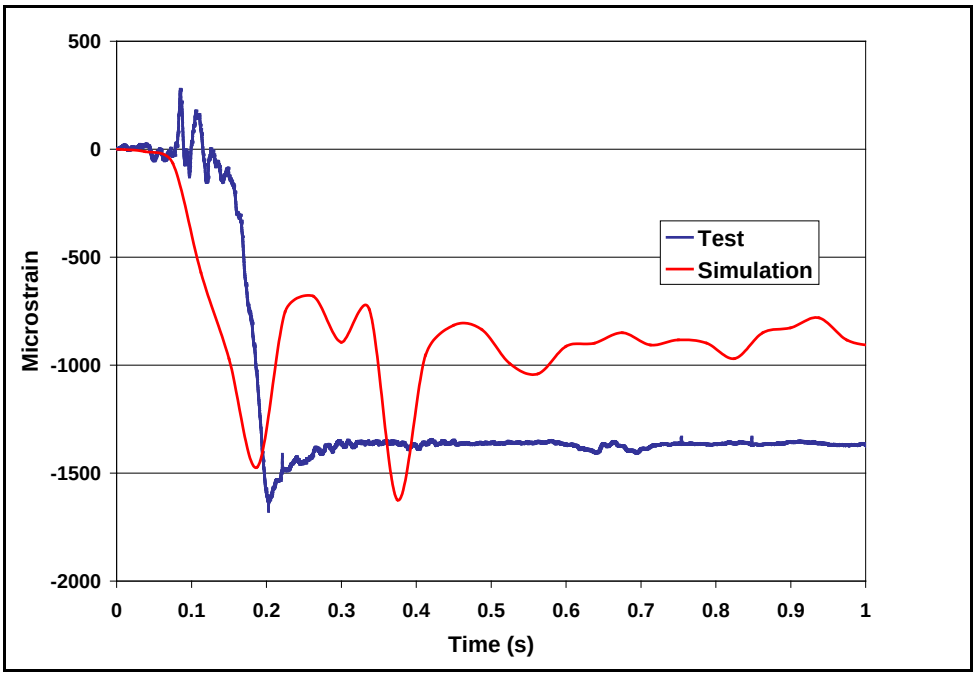

Figure 34. Right Collision Postlongitudinal Strain at Location 10

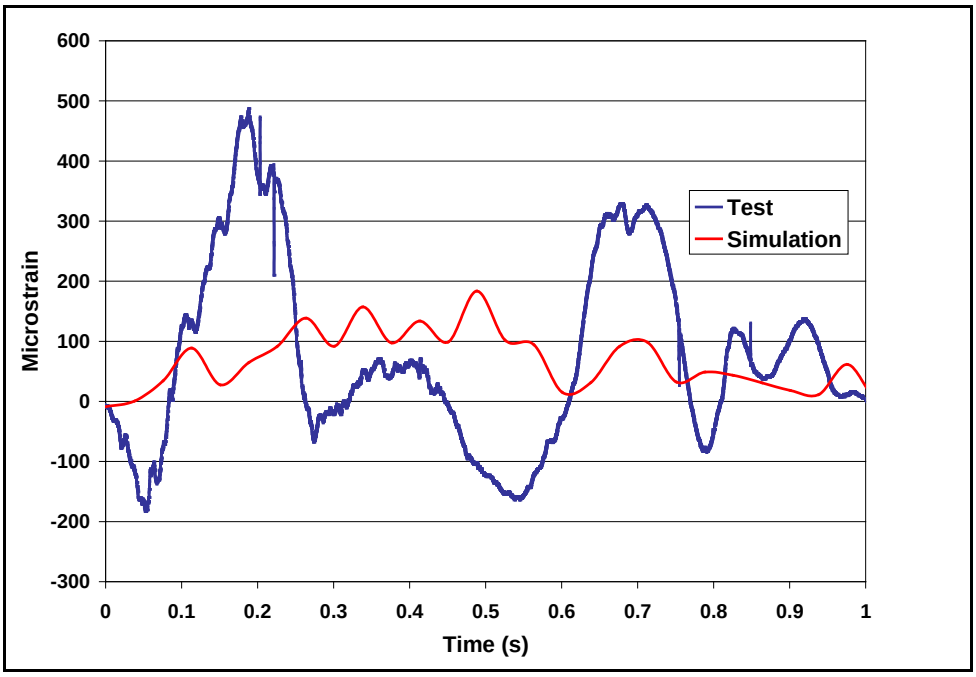

Figure 35. Underframe Longitudinal Strain at Location 2

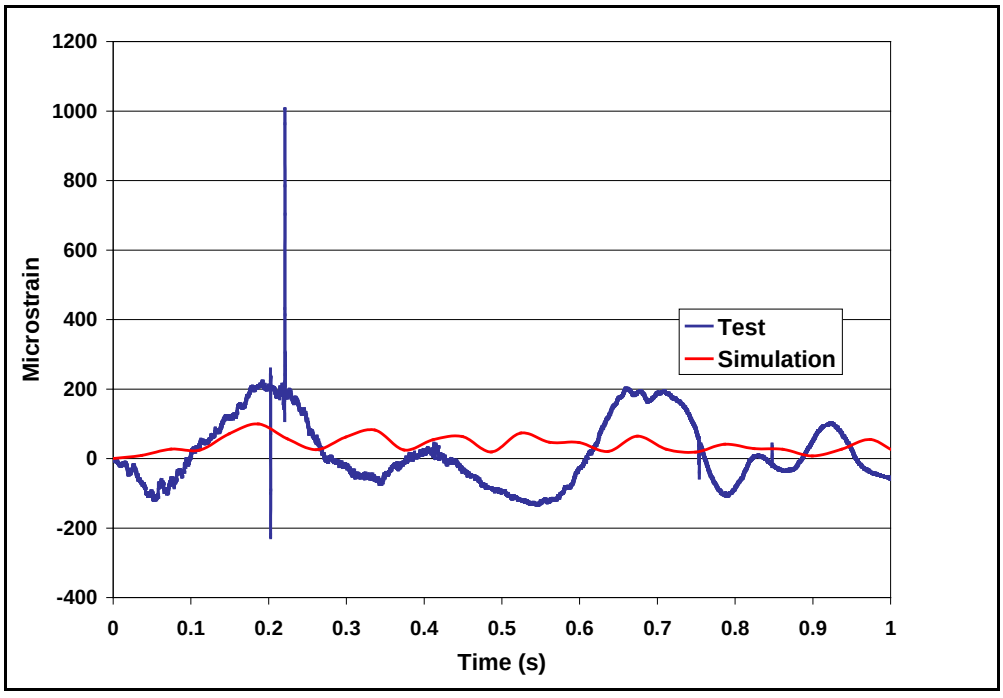

Figure 36. Underframe Longitudinal Strain at Location 6

The above figures show that simulation results are in poor, mixed agreement with the test data on the right collision post for gauge location 1 during the first 0.1 s of the collision locations.

The largest strain on the collision post was 1,800 microstrain. TTCI measured this value on the longitudinal leg of the rosette gauge (location 10) located on the bottom front of the right collision post in the test. The simulation found the largest strain at the same location (location 10) on the right collision post with a value of 1,650 microstrain during the same time frame.

The strains at the top front of the collision posts caused permanent deformation at both collision post locations. The locomotive crashing into hopper cars in the simulation caused the plastic deformation.

3.4 Acceleration Levels on the ATD

TTCI used an instrumented ATD with accelerometers in the engineer's seat of the striking locomotive, as shown in Figure 37, to evaluate the injuries to the crew during the collision.

Figure 37. ATD Position in Cab of Locomotive

From these acceleration measurements, head injury criteria (HIC) were calculated using the standard Equation 1 well known in the literature (Federal Motor Vehicle Safety Standard (FMVSS) No. 208 [6]).

$$HIC = (t_2 - t_1)\left[\frac{1}{t_2 - t_1}\int_{t_1}^{t_2} \alpha_r \, dt\right]^{2.5} \text{----------} \qquad \text{Equation (1)}$$

where α_r = resultant head acceleration in g's.

Table 6 lists injury criteria for the neck, chest, and femur as defined in FMVSS No. 208. Table 6 lists the maximum HIC value, chest acceleration, neck and femur loads imposed on the ATD during the test, and the injury tolerances, along with the direction in which the maximum occurred.

The ATD accelerations and forces are substantially higher than the FMVSS tolerance level for neck force and chest acceleration. During the beginning of the impact event, the unrestrained ATD flailed forward and to the right as the locomotive decelerated and began laterally shifting to the left. At about the same time when the ATD made contact with the right corner post, the

upper corner of the covered hopper car impacted and tore away the right corner post. This violent deformation of the cab corner imparted a large force on the ATD, pushing it back towards the center of the cab and out of the engineer's chair. Figure 38 shows this sequence as the ATD as it hits the cab corner post and gets thrown from the seat.

Table 6. Maximum Forces and g Loads on ATD in Comparison with Injury Tolerances

Parameter	Test	Injury Tolerance
HIC_{15}	1785	700
Neck force (lb)	1353 Vertical	900
Chest acceleration (g)	73 Lateral	60
Femur force (lb)	383 (right leg)	2,250

Figure 38. ATD Impact with Corner Post Sequence

3.5 Assessment

The dynamic sequences predicted by the simulation agreed with the test sequence. The phenomenon of a glancing impact, and most importantly the tearing of the right windshield corner post on the locomotive, occurred in the test and in the simulation.

The strain correlations are reasonably satisfactory at certain locations but poor at others. The strains from the simulation at two points on the right collision post and underframe are in generally good agreement with the measurement in the test regarding the peak value and the time history.

In the case of strain and acceleration simulation data, the difference can likely be attributed to the difference in damage seen to occur on the locomotive and covered hopper car after 0.15 s. The exact track geometry and position of the locomotive and covered hopper car with respect to one another can significantly affect the outcome of this test. A thorough understanding of the wheel-to-rail interaction and accurate modeling of the heavy structural components involved in the collision (i.e., locomotive underframe, vertical end plate, front truck, covered hopper side sills, horizontal end plate, bolster, and front truck) are required to obtain reasonably accurate kinematic results from the simulation.

The destruction of the cab corner pushed back the ATD toward the center of the cab and out of the crew chair.

4. Conclusions

Analysis of the simulation predictions and actual test results leads to the following conclusions:

Structural Damage and Intrusion into Cab Volume

- Significant damage to the corner post area occurred in this test. The intrusion of the cab is a potential for primary injuries to crew.

Correlation between Simulation and Test Results

- The simulations reasonably predicted the overall collision dynamic sequences and damages to the locomotive in all four test scenarios. The model accurately predicted the locomotive override on the colliding hopper.
- The predicted peak deceleration levels showed poor agreement with test data. The deceleration level imposed on the locomotive is an important indicator of the injury potential because of the secondary collision between the crew and interior.
- The time histories in the test and in the simulation differ in the frequency content. The test shows reduced damping and high-frequency content. Peak values of acceleration and strains generally occur within 0.1–0.2 s after impact in the simulation and the test.

5. References

1. Samavedam, G., and Kasturi, K. *Full-Scale Locomotive Dynamic Crash Testing and Correlations Phase I*, draft final report, under review.
2. *HyperMesh User's Manual*, Version 6.0. (2004). Troy, MI: Altair Computing, Inc.
3. *LS-DYNA User's Manual*, Version 96.0. (2004). Livermore, CA: Livermore Software Technology Corporation.
4. *SAE J211-1: Instrumentation for Impact Test—Part 1: Electronic Instrumentation*, Society of Automotive Engineering, Revised 2003.
5. Kasturi, K., and Kokkins, S. *Structural Simulations and Crashworthiness Evaluations of Freight Locomotives in Accidents*, draft final report, under review.
6. *Federal Motor Vehicle Safety Standard No. 208*, Occupant Crash Protection, Title 49 Code of Federal Regulations Section 571.208, Revised October 1999.

Abbreviations and Acronyms

ATD	anthropomorphic test dummy
FMVSS	Federal Motor Vehicle Safety Standard
FEM	finite element model
FRA	Federal Railroad Administration
ft	foot
HIC	head injury criterion
Hz	hertz
in	inch
lb	pound(s)
mph	mile(s) per hour
s	second(s)
TTC	Transportation Technology Center
TTCI	Transportation Technology Center, Inc.